114° with an average H—O—H angle of 107·2°. The corresponding geometrical parameters for the D_2O molecules in $Al(NO_3)_3.9D_2O$ lie within these ranges. The D—O—D angles range from 105·7 (2) to 112·1 (2)° with a mean value of 108·4°, and the O···O···O angles vary between 93·02 (6) and 118·09 (6)°.

Fig. 4 gives a plot of O—D *versus* D···O distances. It shows the same trend as other correlation curves published for O—H···O hydrogen bonds (see, for example, Olovsson & Jönsson, 1976) and gives an indication of the quality of the present results.

I wish to thank Professor Ivar Olovsson for the facilities he has placed at my disposal. I am also indebted to Dr Roland Tellgren for valuable assistance with the data collection and to Dr John O. Thomas for many stimulating discussions.

This work has been supported by grants from the Swedish Natural Science Research Council which are gratefully acknowledged.

References

ABRAHAMS, S. C. & KEVE, E. T. (1971). *Acta Cryst.* A**27**, 157–165.
BECKER, P. & COPPENS, P. (1975). *Acta Cryst.* A**31**, 417–425.
CHIARI, G. & FERRARIS, G. (1982). *Acta Cryst.* B**38**, 2331–2341.
FALK, M. & KNOP, O. (1973). *Water. A Comprehensive Treatise*, Vol. 2, edited by F. Franks, pp. 80–85. New York: Plenum.
GUSTAFSSON, T., LUNDGREN, J.-O. & OLOVSSON, I. (1980). *Acta Cryst.* B**36**, 1323–1326.
HERMANSSON, K., THOMAS, J. O. & OLOVSSON, I. (1980). *Acta Cryst.* B**36**, 1032–1040.
HERPIN, P. & SUDARSANAN, K. (1965). *Bull. Soc. Fr. Minéral. Cristallogr.* **88**. 595–601.
JOHNSON, C. K. (1969). *Acta Cryst.* A**25**, 187–194.
KOESTER, L. & STEYERL, A. (1977). *Neutron Physics*, p. 36. Berlin, Heidelberg, New York: Springer.
LEHMANN, M. S. & LARSEN, F. K. (1974). *Acta Cryst.* A**30**, 580–584.
LUNDGREN, J.-O. (1982). *Crystallographic Computer Programs*. Report UUIC-B13-04-05. Institute of Chemistry, Univ. of Uppsala.
OLOVSSON, I. & JÖNSSON, P.-G. (1976). *The Hydrogen Bond*, edited by P. SCHUSTER, G. ZUNDEL & C. SANDORFY, pp. 393–456. Amsterdam: North-Holland.
THORNLEY, F. R. & NELMES, R. J. (1974). *Acta Cryst.* A**30**, 748–757.

Acta Cryst. (1983). C**39**, 930–936

The Structure and Electron Deformation Density of $LiNO_2.H_2O$ at 295 K

BY KERSTI HERMANSSON AND JOHN O. THOMAS

Institute of Chemistry, University of Uppsala, Box 531, *S*-751 21 *Uppsala, Sweden*

(*Received* 20 *December* 1982; *accepted* 5 *April* 1983)

Abstract. $M_r = 70·959$, monoclinic, $P2_1/c$, $Z = 4$, $a = 3·3387$ (3), $b = 14·2980$ (10), $c = 6·3961$ (5) Å, $\beta = 105·10$ (1)°, $V = 294·79$ (4) Å^3, $D_x = 1·60$ Mg m^{-3}, Mo $K\alpha$, $\lambda = 0·71069$ Å, $\mu_{calc} = 0·154$ mm^{-1}, $T = 295$ K, $F(000) = 144$. Two data sets were collected out to $\sin\theta/\lambda = 0·91$ Å^{-1}: one on a twinned crystal, the other on a single crystal. Positional and thermal parameters from the two data sets show only random deviations. Somewhat high $R_w(F^2)$ values of 0·084 and 0·081, respectively, resulted from the refinement of a spherical-atom model. This reflects the inadequacies of such a model. Introduction of multipolar deformation functions for the single-crystal data set brought the $R_w(F^2)$ value down to 0·029. The crystal contains one independent Li^+ ion with fivefold coordination, a tetrahedrally coordinated H_2O molecule and an NO_2^- ion which accepts two medium-strength hydrogen bonds [O—H···O 2·755 (1); O—H···N 2·890 (1) Å] and has three Li^+—O contacts. The static deformation density for the NO_2^- ion shows N—O bond maxima of 0·50 e Å^{-3}; O lone-pair maxima of 0·20–0·30 e Å^{-3} are situated in the molecular planes at approximately 90° to the N—O bonds. The lone-pair density associated with the water O is markedly asymmetric; no support for this effect has been found in theoretical model calculations, however.

Introduction. Electron density studies of a series of hydrates are underway at this Institute. $LiNO_2.H_2O$ has a high valence/core electron ratio, $V/\sum n^2_{core} = 3·7$ (Stevens & Coppens, 1976) and is, at least in this respect, well suited to electron density study. Moreover, its constituent ions and molecules are similar to those of $LiNO_3.3H_2O$, previously studied in this project (Hermansson, Thomas & Olovsson, 1977).

Two X-ray data sets were collected. Twinned crystals are readily formed and, unwittingly, our first data set was collected on such a crystal. The structure was solved from these data. The results from this refinement were, in fact, of the same quality (judged on the basis of R values, σ's, *etc.*) as those from a second untwinned data set which was collected later. Tables of coordinates and distances refer to the untwinned data set.

0108-2701/83/080930—07$01.50

Experimental. The cell dimensions were determined from 21 lines on a powder photograph taken on a Guinier–Hägg focusing camera at 295 K with Cr $K\alpha_1$ radiation. The monoclinic cell can be regarded as *B*-centred pseudo-orthorhombic; hence the predisposition for twinning in the structure (see below). Crystals were grown by cooling a warm, saturated solution of $LiNO_2$, which had been prepared by mixing aqueous solutions of $AgNO_2$ and LiCl. The crystals are hygroscopic. The crystals readily grow as twins; the twinned cells are related by a mirror plane perpendicular to **a**. Weissenberg photographs from twinned crystals in many cases showed close to orthorhombic symmetry, confirming Ziegler's (1935) findings. All but the *h*0*l* reflections contain contributions from both the *hkl* reflection of the first twin type and the *h,k,*−*h*−*l* reflection of the second twin type. A 50%–50% occurrence of the two twin components thus results in an apparent orthorhombic symmetry.

Structure solution on twinned crystal. Crystal of volume 9×10^{-3} mm^3, Stoe–Philips four-circle diffractometer, 2150 unique reflections, $\sin\theta/\lambda \leq 0{\cdot}91$ Å^{-1}; direct methods in space group $P2_1$ (*MULTAN*, Declercq, Germain, Main & Woolfson, 1973); all non-H atoms located in the *E* maps, least-squares refinement (*UPALS*, Lundgren, 1982), H from ΔF maps, $R(F) = 0{\cdot}18$ for 1431 reflections with $F_o^2 > 2\sigma(F_o^2)$. Resulting positions differed by approximately 0·10 Å from the positions obtained subsequently from the single-crystal data set.

A structure refinement using the twinned data set was carried out in space group $P2_1/c$ and with the inclusion of a refinable parameter κ such that

$$F_{c,\mathrm{tot}}^2(hkl) = \kappa F_c^2(hkl) + (1-\kappa)F_c^2(h,k,-h-l).$$

The refined value for κ was 0·641 (2), in good agreement with our estimated value of 0·64 (1) from the *h*0*l* intensities. The final $R_w(F^2)$ value was 0·084 for all 1950 reflections with $F_o^2 > 0{\cdot}0$ and 0·078 for the 1431 reflections with $F_o^2 > 2\sigma(F_o^2)$.

Data collection and reduction of the single-crystal data set. Parallelepiped, volume 5×10^{-3} mm^3 (maximum dimension 0·2 mm), sealed in glass capillary; Enraf–Nonius CAD-4 diffractometer, graphite-monochromatized Mo $K\alpha$ radiation; *h*0*l*, $l \neq 2n$ reflections extinct, indicating an untwinned crystal with space group $P2_1/c$; 6400 reflections, $h \pm k \pm l$, $\sin\theta/\lambda \leq 1{\cdot}05$ Å^{-1}, continuous scanning, scan range $\Delta\theta = 1{\cdot}0° + 0{\cdot}35° \tan\theta$; reflections $\sin\theta/\lambda > 0{\cdot}91$ Å^{-1} discarded as being too weak. As a check on multiple scattering, reflections for which $0 < \sin\theta/\lambda < 0{\cdot}70$ Å^{-1} were measured at three different ψ angles, 1° apart, and with the time for each measurement divided by three. A deviation in excess of $3\sigma_c$ from the weighted average intensity occurred for only 25 of the reflections measured (σ_c is the standard deviation for the average intensity based on Poisson counting statistics); no deviation was larger than $5\sigma_c$. All eight test reflections monitored throughout the data collection showed similar behaviour (an intensity increase of 1·5–2% during the first 200 h of irradiation, and a subsequent decrease of 2·5–3·0% over the last 300 h); the whole data set was scaled accordingly. A profile-analysis method (Lehmann & Larsen, 1974) was used in making the background correction; the integrated intensities were corrected for Lorentz, polarization and absorption effects (the latter was superfluous, however, since μ_{calc} is 0·154 mm^{-1} and the transmission factors vary between 0·974 and 0·979). 99·9% of all symmetry-equivalent reflections, *hkl* and $h\bar{k}l$, agreed within $3\sigma_c$; their average was taken. Some 100 extinct reflections which had been measured as a check on the space group were also removed, leaving in total 1849 reflections.

Conventional refinement from single-crystal data. The preliminary atomic parameters obtained from the least-squares refinement of the twinned-crystal data set were used as input parameters in the new least-squares refinement cycles (using the program *UPALS*). The quantity refined was $\sum w(F_o^2 - kF_c^2)^2$ where $w^{-1} = \sigma_c^2(F_o^2) + (kF_o^2)^2$. The constant k was set empirically to 0·03, which made the quantity $\langle w(F_o^2 - F_c^2)^2 \rangle$ roughly equal for different intensity groups. In the final cycles of refinement, one scale factor, one isotropic extinction parameter, positional and anisotropic thermal parameters for the non-hydrogen atoms and positional and isotropic thermal parameters for the H atoms were refined. The data set was only slightly affected by extinction; two reflections were weakened by more than 5%. All reflections except 002 (weakened by 20%) were included in the refinement. The scattering factors and anomalous-dispersion corrections used for H, Li^+, N and O were taken from *International Tables for X-ray Crystallography* (1974, pp. 72–73 and 149). The final $R_w(F^2)$ value was 0·081 for a refinement when all 1375 reflections with $F_o^2 > 0$ were included and 0·077 for the 1007 reflections with $F_o^2 > 2\sigma(F_o^2)$. The corresponding unweighted *R* values were 0·048 and 0·041.

Table 1. *Atomic positional parameters* (× 10^5) *and equivalent isotropic thermal parameters* (*expressed as the average r.m.s. amplitude*)

The first row refers to the spherical-atom refinement and the second to the deformation refinement of the single-crystal data set.

	x	*y*	*z*	*U*(Å)
N	76557 (23)	36019 (4)	28127 (11)	0·166
	76545 (34)	35995 (6)	28070 (13)	0·165
O(1)	64384 (21)	28304 (4)	19283 (9)	0·180
	64257 (30)	28279 (5)	19208 (12)	0·179
O(2)	79936 (29)	42241 (4)	15092 (9)	0·181
	79973 (30)	42253 (5)	15022 (12)	0·180
O(*W*)	8226 (20)	39106 (4)	74114 (9)	0·169
	8102 (35)	39123 (6)	74076 (12)	0·163
Li	36029 (49)	83273 (10)	62982 (22)	0·176
	36017 (44)	83274 (8)	63004 (18)	0·169
H(1)	9544 (374)	44737 (107)	76061 (189)	0·142
	9907*	45832*	76426*	0·210*
H(2)	391 (363)	38476 (82)	61491 (207)	0·132
	−2289*	38211*	58572*	0·210*

* Not refined (see text).

After the refinement with all reflections with $F_o^2 > 0$ included, there were 44 reflections with $|F_o^2 - F_c^2|/\sigma(F_o^2)$ values greater than 3·0; amongst these, 15 values were greater than 5·0. The δR plot was slightly S shaped with slope 0·82 and y intercept −0·18. The residual density map after the last cycle of refinement contained systematic features in the bonding and lone-pair regions, with peak heights up to ~ 0·25 e Å^{-3}. The final atomic positions are listed in Table 1.*

The results from the twinned-crystal and the single-crystal data sets are of comparable quality. The regular spherical-atom refinements with the two data sets give standard deviations which are, in general, the same within ± 10% for corresponding parameters. The resulting distances are the same within two combined standard deviations.

Deformation refinements from single-crystal data. Deformation density refinements were carried out in which a number of multipole deformation functions with Gaussian radial dependence were centred on each atom. The coefficients (occupancies) for each of these functions were refined together with the normal parameters of a least-squares refinement. The type of deformation functions employed is that given by Hirshfeld (1971). Several deformation models were attempted. Although all atoms are situated in general positions in the unit cell, mirror planes were at first imposed on the deformation functions of the NO_2^- ion and H_2O molecule [even *mm* site symmetry for N and O(*W*)]. These symmetries were gradually lowered, which resulted in significant improvements in the model. In the last cycle of refinement, no extra symmetry was imposed on the non-hydrogen atoms, but the hydrogen deformation density functions were restricted to be cylindrically symmetric around the H—O(*W*) bonds. Moreover, the deformation coefficients on O(1) and O(2) and H(1) and H(2) were constrained to be equal (removal of these constraints made no significant improvement to the model). Deformation coefficients up to the octapolar level were refined for N, O(1), O(2) and O(*W*), and up to the quadrupolar level for Li^+, H(1) and H(2) (79 coefficients in all). In all, 120 parameters were refined as compared to 55 for the spherical-atom refinement. The two H atoms were fixed at positions derived from the spherical-atom refinement by lengthening the O(*W*)—H(1) and O(*W*)—H(2) distances to 0·970 Å. The isotropic thermal parameters were fixed to 3·5 Å^2 for both H atoms. We also tested a model in which the O(*W*)—H distances were set to 1·0 Å. All refined parameters agreed to within one combined σ with those from the previous refinements. The effect of the H-atom positions on the deformation density maps will be discussed later.

The final $R_w(F^2)$ value was 0·029 for all reflections with $F_o^2 > 0$ and 0·027 for reflections with $F_o^2 > 2\sigma(F_o^2)$. The δR plot was a straight line with slope 1·00 and intercept −0·18 for the refinement including all reflections with $F_o^2 > 0$. Standard deviations on positional and thermal parameters increased by approximately 15% when only the reflections with $F_o^2 > 2\sigma(F_o^2)$ were included in the refinement. The weights used in the deformation refinements were $1/\sigma^2(F_o^2)$ where $\sigma^2(F_o^2) = \sigma_c^2(F_o^2) + (0{\cdot}01F_o^2)^2$. Only nine reflections had $|F_o^2 - F_c^2|/\sigma(F_o^2)$ values greater than 3·0 and one greater than 5·0 after the deformation refinement. The ratio between the scale factors (on $|F_o|$) from the deformation and spherical-atom refinements was 1·015.

The standard deviations of the positional parameters resulting from the deformation refinement were approximately 35% higher, and the standard deviations of the thermal parameters 15% lower than those of the spherical-atom refinement. The atomic positions resulting from the deformation refinement (given in Table 1) differ from the spherical-atom refinement results by 0·005 (1), 0·007 (1), 0·005 (1), 0·005 (1), and 0·002 (2) Å for N, O(1), O(2), O(*W*) and Li^+, respectively. The vectors from the spherical-atom positions towards the deformation refinement positions point roughly towards the lone-pair direction for N and O(*W*) and towards the N atom for O(1) and O(2). The ratios of the thermal parameters, U_{ii} (def. ref.)/U_{ii} (spherical-atom ref.), vary between 0·92 and 1·03.

Discussion. Distances and angles resulting from the deformation refinement are listed in Table 2.

Table 2. *Interatomic distances* (Å) *and angles* (°) *resulting from the deformation refinement of the single-crystal data set*

Li^+—O(1)	2·007 (1)	O(1)—Li^+—O(1′)	105·47 (5)
Li^+—O(*W*)	2·015 (2)	O(1)—Li^+—O(2)	157·62 (7)
Li^+—O(*W*′)	2·046 (2)	O(1)—Li^+—O(*W*)	104·45 (7)
Li^+—O(2)	2·156 (1)	O(1)—Li^+—O(*W*′)	89·85 (6)
Li^+—O(1′)	2·178 (1)	O(1′)—Li^+—O(2)	57·98 (4)
		O(1′)—Li^+—O(*W*)	107·42 (7)
		O(1′)—Li^+—O(*W*′)	133·63 (7)
		O(2)—Li^+—O(*W*′)	92·52 (6)
		O(*W*)—Li^+—O(*W*′)	110·60 (6)
N—O(1)	1·259 (1)	O(1)—N—O(2)	113·75 (8)
N—O(2)	1·249 (1)		
O(*W*)—H(1)	0·970*	H(1)—O(*W*)—H(2)	106·4*
O(*W*)—H(2)	0·970*	O(2)—O(*W*)—N	113·43 (3)
O(*W*)—H(1)···O(2)	2·755 (1)	Li^+—O(*W*)—$Li^{+\prime}$	110·60 (6)
O(*W*)—H(2)···N	2·890 (1)	Li^+—O(*W*)—N	113·98 (3)
		Li^+—O(*W*)—O(2)	103·89 (5)
		$Li^{+\prime}$—O(*W*)—O(2)	111·38 (5)
		$Li^{+\prime}$—O(*W*)—N	103·78 (5)

* In the spherical-atom refinement, where the H parameters were also refined, the resulting O(*W*)—H(1) and O(*W*)—H(2) distances were 0·81 (2) and 0·79 (1) Å, respectively, and the H(1)—O(*W*)—H(2) angle was 105·1 (11)°.

* The final thermal parameters and lists of structure factors resulting from both the spherical-atom and the deformation refinements have been deposited with the British Library Lending Division as Supplementary Publication No. SUP 38485 (58 pp.). Copies may be obtained through The Executive Secretary, International Union of Crystallography, 5 Abbey Square, Chester CH1 2HU, England.

The structure

A stereoscopic illustration of the structure is given in Fig. 1. It is seen to comprise a three-dimensional network. The NO_2^- ions and the H_2O molecules form approximately planar ring systems, with medium-strength hydrogen bonds running roughly in the **b** and **c** directions.

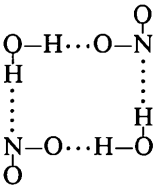

The Li^+ *ion.* The Li^+ ion is surrounded by five O atoms belonging to two H_2O molecules and two NO_2^- ions; one NO_2^- neighbour thus forms a bidentate and the other a monodentate O—Li^+ contact. A large number of structures containing NO_2^- ions have been published. In some of these, all the NO_2^- ions surrounding the cation form bidentate and/or monodentate cation–oxygen contacts; in others one finds only cation–nitrogen contacts. A mixture of these two arrangements is also common. The Li^+—O distances lie in the range 2·007–2·178 Å with a mean value of 2·080 Å. In a limited survey of Li—O bond lengths for four-, five- and sixfold coordination (Hermansson, Thomas & Olovsson, 1977), a mean value of 2·077 Å was found for fivefold coordination.

The NO_2^- *ion.* The NO_2^- ion accepts two hydrogen bonds [O(*W*)—H(1)···O(2) and O(*W*)—H(2)···N] and binds to two Li^+ ions through three O—Li^+ contacts. The N—O(1) and N—O(2) bond distances are 1·259 (1) and 1·249 (1) Å, respectively, and the O(1)—N—O(2) angle is 113·75 (6)°. These values are in agreement with the geometries of other crystalline NO_2^- ions studied by diffraction [see Abrahams, Bernstein & Liminga (1980) for a brief review]. The bond difference of 0·010 (1) Å seems to reflect a stronger intermolecular bonding to O(1); it participates in two Li^+—O bonds while O(2) has one Li^+—O contact and acts as an acceptor of one hydrogen bond.

For $Ba(NO_2)_2.H_2O$, studied by neutron diffraction at three temperatures, Kvick, Liminga & Abrahams (1982) found that at 298 K the two N—O bonds within one NO_2^- ion differed by 0·010 (2) Å and in the other independent NO_2^- ion by 0·015 (1) Å. These rather large differences within each ion were partly due to effects of different thermal motion for the O atoms and decreased to 0·008 (1) and 0·007 (1) Å at 20 K, where the diffraction-determined bond distances are less affected by apparent foreshortening due to thermal motion. Since the vibrational ellipsoids for O(1) and O(2) in $LiNO_2.H_2O$ are very similar, the observed difference of 0·010 (1) Å between the N—O(1) and N—O(2) bond lengths is less likely to disappear on cooling.

The H_2O *molecule and hydrogen bonds.* The H_2O molecule has approximately regular tetrahedral surroundings, serving as hydrogen-bond donor to two NO_2^- ions and having two Li^+—O contacts. The hydrogen bonds are of intermediate strength {O(*W*)—H(1)···O(2) 2·755 (1) Å; O(*W*)—H···N 2·890 (1) Å [the average value reported by Chiari & Ferraris (1982) for O(*W*)···O bonds in hydrates is 2·805 Å]}.

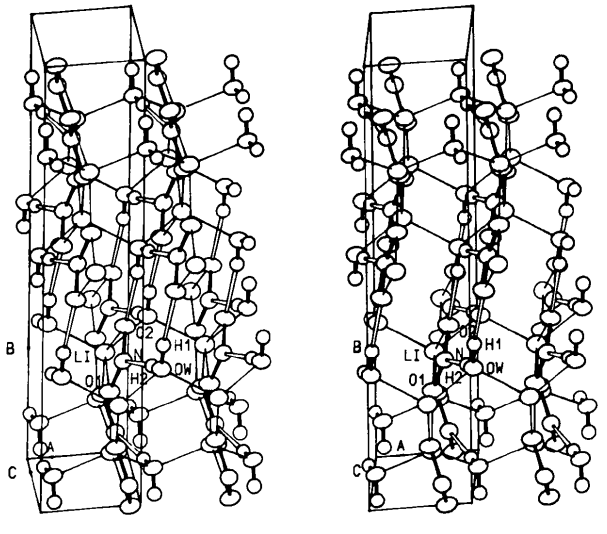

Fig. 1 A stereoscopic illustration of the structure of $LiNO_2.H_2O$. The thermal ellipsoids are drawn to include 50% probability.

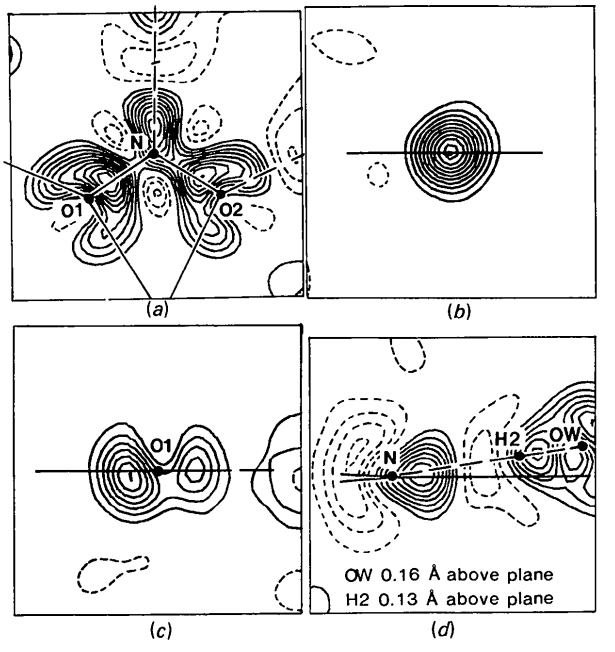

Fig. 2. The static deformation electron density of the NO_2^- ion. The contour interval in Figs. 2 and 3 is 0·05 e $Å^{-3}$. Negative contours are dashed and the zero contour is omitted. (*a*) In the NO_2^- plane. (*b*) Perpendicular to the N—O(1) bond, at 0·40 Å from O(1) and 0·86 Å from N (the molecular plane is indicated in *b*–*d*). (*c*) Perpendicular to the N—O(1) bond, through the O(1) nucleus. (*d*) In a plane bisecting the O(1)—N—O(2) angle.

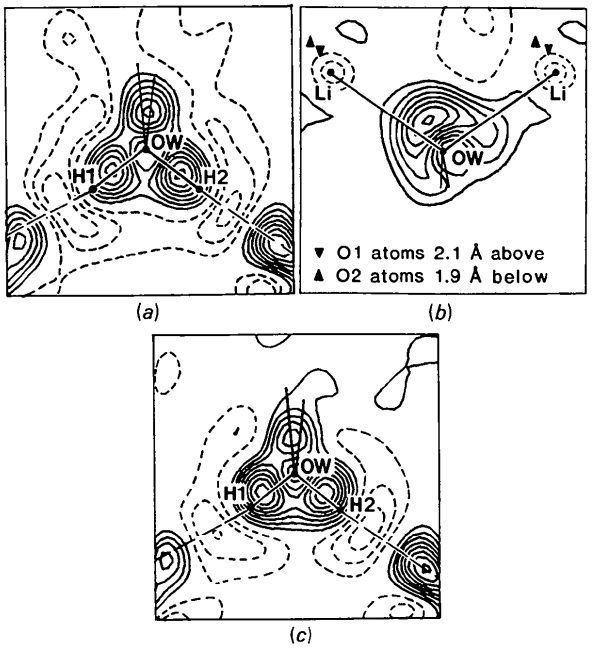

Fig. 3. The static deformation density for the H_2O molecule. (*a*) In the molecular plane. (*b*) In the Li^+—O(*W*)—Li^+ plane. (*c*) Same section as in (*a*) but with the density derived from a deformation refinement based on a different set of H positional and thermal parameters (see text).

The deformation electron density

The static deformation density for the NO_2^- ion and the H_2O molecule is shown in Figs. 2–3. This density has been calculated from the refined deformation coefficients and the corresponding density functions by means of a double Fourier synthesis procedure including *all* reflections out to $\sin\theta/\lambda = 1{\cdot}05$ Å^{-1}. The atomic reference states in the maps are the ground-state spherically averaged static electron densities of N, O, H and Li^+.

The NO_2^- *ion.* The deformation density in the molecular plane is shown in Fig. 2(*a*). The prominent features are large N—O bond peaks, electron excess in the lone-pair regions of the O atoms at approximately 90° to the N—O bonds, and one well developed lone-pair peak on N. The maximum *static* deformation densities in the N—O bonds are 0·50 and 0·45 e Å^{-3} (0·30–0·35 e Å^{-3} for the *dynamic* density). This result is in contrast to some previous electron density studies of compounds containing N—O bonds, where negligible or only very weak N—O bond peaks have been observed: uronium nitrate (Harkema, 1971), *p*-nitropyridine *N*-oxide (Coppens & Lehmann, 1976), $LiNO_3.3H_2O$ (Hermansson, Thomas & Olovsson, 1983). On the other hand, maximum peak densities of about 0·30 e Å^{-3} were found in the N—O bonds of $K_2Na[Co(NO_2)_6]$ (Ohba, Toriumi, Sato & Saito, 1978) and $NaNO_3$ (Göttlicher & Knöchel, 1980); for the three N—O bonds in $S_4N_3NO_3$ (Moss, Guru Row & Coppens, 1980), the peak heights varied between 0·08 and 0·42 e Å^{-3}. Several theoretical semi-empirical and *ab initio* SCF and CI calculations have been carried out on NO_2^-; few of these deal with the electron density distribution, however. Ohba *et al.* (1978) performed CNDO/2 calculations on a free NO_2^- ion using the atomic positions from $K_2Na[Co(NO_2)_6]$; no positive peak was observed in the N—O bonding region. *Ab initio* SCF calculations on NO_3^- (de With, Feil & Baerends, 1975) show no excess density in the N—O bonds. A section perpendicular to the N—O(1) bond approximately through the bond maximum [at 0·40 Å from the O(1) nucleus] in Fig. 2(*b*) shows no evidence of π bonding in the form of elongation of the bond peak perpendicular to the NO_2^- plane. This is also true for the N—O(2) bond density. The lone-pair peaks of O(1) and O(2) are not well resolved from the N—O bond peaks. Nevertheless, it is seen from Fig. 2(*a*) that the lone-pair peaks are situated at about 0·45 Å from the O nucleus and at approximately right-angles to the N—O bonds. A section through the O(1) atom perpendicular to the N—O(1) bond is shown in Fig. 2(*c*). The O lone-pair features for $LiNO_2.H_2O$ agree with the results for uronium nitrate, *p*-nitropyridine *N*-oxide and $S_4N_3NO_3$ (see earlier references). The lone-pair density of the N atom is displayed in Fig. 2(*d*) in a plane bisecting the O(1)—N—O(2) angle. There is no significant tendency for the lone-pair density to orient itself towards the incoming O(*W*)—H···N hydrogen bond which makes an angle of 8° with the NO_2^- plane. (The maximum of this lone-pair peak does not move for a deformation refinement including only reflections out to $\sin\theta/\lambda = 0{\cdot}80$ Å^{-1}.) A distortion of the lone-pair density from mirror-plane symmetry in the form of a polarization towards the side of the molecule which accepts the short hydrogen bond has been observed for the H_2O oxygen atom in $C_2H_2O_4.2H_2O$ (Stevens & Coppens, 1980). A similar effect, although more pronounced, was observed for two independent H-bond-accepting C—O⁻H groups in $C_8H_{16}O_2.\frac{1}{2}H_2O$ (van der Wal & Vos, 1979). There are also several examples in the literature of the opposite effect, *i.e.* a decrease of O lone-pair electron density due to hydrogen bonding. This has been observed both experimentally [see Eisenstein (1979) and references therein] and theoretically [see references in Hermansson & Lunell (1981)].

The section displayed in Fig. 2(*d*) almost coincides with the hydrogen bond. The O(*W*)—H···N bond thus shows the typical features observed for medium-strength O—H···O bonds: electron deficiency on the weakly bonded side of the H atom and electron excess in the O—H bond and in the lone-pair region of the hydrogen-bond acceptor.

Even though it should be borne in mind that both 'experimental' atomic charges obtained from a deformation refinement and theoretical charges from a Mulliken population analysis are subject to a high degree of arbitrariness, it may be interesting to compare the atomic charges for the NO_2^- ion in $LiNO_2.H_2O$ with

theoretical calculations on a free NO_2^- ion. For three different theoretical calculations, two *ab initio* SCF calculations (Pearson, Schaefer, Richardson, Stephenson & Brauman, 1974; Pullman & Berthod, 1981), and one CNDO/2 calculation (Ohba, Toriumi, Sato & Saito, 1978), the charge on N varied between +0·02 and +0·17 and the charge on O between −0·51 and −0·58. The geometry of the NO_2^- ion used in these calculations was 1·25 ± 0·01 Å for the N—O distance and 117 ± 2° for the O—N—O angle. The experimental charges obtained for the NO_2^- ion in $LiNO_2.H_2O$ (present work) are + 0·51 for the N atom and −0·67 for the O atoms [the same value for O(1) and O(2) because of the constraints imposed on the deformation model]. This result indicates an increased polarization of the NO_2^- ion due to the influence of the environment.

The H_2O *molecule.* The *static* deformation density of the H_2O molecule is displayed in the molecular plane in Fig. 3(*a*) and in the Li^+—O(*W*)—Li^+ plane in Fig. 3(*b*). The O—H bond-density maxima are 0·30—0·35 e Å^{-3} (or 0·20—0·25 e Å^{-3} for the dynamic density). The electron-deficient regions on the weakly bonded side of the H atoms have minima of −0·15 e Å^{-3}. The lone-pair density of O(*W*) is clearly unsymmetrical with respect to a plane bisecting the Li^+—O(*W*)—Li^+ angle (Fig. 3*b*): the maximum electron density in the directions of the two Li^+—O(*W*) contacts are 0·15 and 0·30 e Å^{-3}, respectively (0·10 and 0·20 e Å^{-3}, for the dynamic density). The two Li^+—O(*W*) distances are quite similar (2·015 and 2·046 Å). The next-nearest neighbours are two nitrite O atoms at distances of 2·862 and 3·037 Å on the side of the weakly developed lone-pair density, and two nitrite O atoms further away [at 3·089 and 3·179 Å from O(*W*)] on the other side. In view of the relatively high negative charge on the O atoms in NO_2^-, we wanted to ascertain whether the unsymmetrical environment around the O(*W*) atom could be the reason for the asymmetrical lone-pair density. To this end a quantum-mechanical *ab initio* MO–LCAO–SCF calculation was carried out on a system consisting of an H_2O molecule (same geometry as in $LiNO_2.H_2O$) with the crystal environment of $LiNO_2.H_2O$ simulated by point charges placed at the diffraction-determined atomic positions out to a distance of 6·0 Å from O(*W*).* The point charges (73 in all) were taken from the result of the deformation refinement. This model is certainly a crude approximation to the true crystal; it should suffice, however, to give an indication of the order of magnitude of the effects one might expect from the crystal field. Fig. 4 shows the theoretical difference density where the electron density of a free H_2O molecule (calculated in the same geometry and with the same basis sets) has been subtracted from the density of the entire model system.

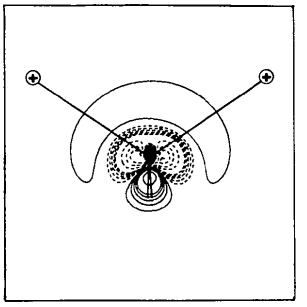

Fig. 4. Static theoretical deformation density in the cation—O(*W*)—cation plane showing $\rho(H_2O$ + point charges)$-\rho(H_2O)$. The two closest positive neighbours are indicated in the map. The contours are ±0·01, ±0·02, ···, ±0·05, ±0·10, ··· e Å^{-3}.

The conclusion is that the O(*W*) lone-pair asymmetry obtained experimentally can hardly be caused by the asymmetry of the crystalline environment. It would be interesting to see whether this lone-pair asymmetry is reproduced in a low-temperature experimental study.

Fig. 3(*c*) has been derived from a deformation refinement where the O(*W*)—H(1) and O(*W*)—H(2) bonds were fixed at 1·0 Å instead of 0·97 Å (as was the case for the results presented in Figs. 2 and 3*a*–*b*) and the isotropic thermal parameter was fixed to 2·5 Å^2 instead of 3·5 Å^2. In all other respects, the refinements were identical. The similarity between Figs. 3(*a*) and 3(*c*) illustrates the important result that an exact knowledge of the H parameters (from neutron data) may not be crucial to a meaningful density analysis (see also Stevens, Rys & Coppens, 1978). The deformation electron density for the NO_2^- ion was almost identical for the two refinements.

We wish to thank Professor I. Olovsson for the facilities placed at our disposal. We are also indebted to Mr H. Karlsson for growing the crystals and to Dr T. Gustafsson for assistance with one of the data collections. This work has been sponsored by the Swedish Natural Science Research Council.

* The program system *MOLECULE* (Almlöf, 1972) was used for the calculation of the wavefunctions. The basis sets used were Dunning's (1970) (9*s*5*p*/4*s*) set contracted to < 4*s*2*p*/2*s*> with one polarization function on both O and H.

References

ABRAHAMS, S. C., BERNSTEIN, J. L. & LIMINGA, R. (1980). *J. Chem. Phys.* **72**(11), 5837–5862.
ALMLÖF, J. (1972). USIP Rep. 72–09. Univ of Stockholm, Sweden.
CHIARI, G. & FERRARIS, G. (1982). *Acta Cryst.* B**38**, 2331–2341.
COPPENS, P. & LEHMANN, M. S. (1976). *Acta Cryst.* B**32**, 1804–1809.
DECLERCQ, J. P., GERMAIN, G., MAIN, P. & WOOLFSON, M. M. (1973). *Acta Cryst.* A**29**, 231–234.
DUNNING, T. H. (1970). *J. Chem. Phys.* **53**, 2823–2833.
EISENSTEIN, M. (1979). *Acta Cryst.* B**35**, 2614–2625.
GÖTTLICHER, S. & KNÖCHEL, C. D. (1980). *Acta Cryst.* B**32**, 1777–1784.
HARKEMA, S. (1971). Thesis. Twente Univ. of Technology, Enschede, The Netherlands.
HERMANSSON, K. & LUNELL, S. (1981). *Chem. Phys. Lett.* **80**, 64–68.
HERMANSSON, K., THOMAS, J. O. & OLOVSSON, I. (1977). *Acta Cryst.* B**33**, 2857–2861.

HERMANSSON, K., THOMAS, J. O. & OLOVSSON, I. (1983). To be published.
HIRSHFELD, F. L. (1971). *Acta Cryst.* B**27**, 769–781.
International Tables for X-ray Crystallography (1974). Vol. IV. Birmingham: Kynoch Press.
KVICK, Å., LIMINGA, R. & ABRAHAMS, S. C. (1982). *J. Chem. Phys.* **76**, 5508–5514.
LEHMANN, M. S. & LARSEN, F. K. (1974). *Acta Cryst.* A**30**, 580–584.
LUNDGREN, J.-O. (1982). Report UUIC-B13-04-05. Institute of Chemistry, Univ. of Uppsala.
MOSS, G., GURU ROW, T. N. & COPPENS, P. (1980). *Inorg. Chem.* **19**, 2396–2403.
OHBA, S., TORIUMI, K., SATO, S. & SAITO, Y. (1978). *Acta Cryst.* B**34**, 3535–3542.
PEARSON, P. K., SCHAEFER, H. F. III, RICHARDSON, Y. H., STEPHENSON, L. M. & BRAUMAN, J. I. (1974). *J. Am. Chem. Soc.* **96**, 6778–6779.
PULLMAN, A. & BERTHOD, H. (1981). *Chem. Phys. Lett.* **81**, 195–200.
STEVENS, E. D. & COPPENS, P. (1976). *Acta Cryst.* A**32**, 915–917.
STEVENS, E. D. & COPPENS, P. (1980). *Acta Cryst.* B**36**, 1864–1876.
STEVENS, E. D., RYS, J. & COPPENS, P. (1978). *J. Am. Chem. Soc.* **100**, 2324–2328.
WAL, H. R. VAN DER & VOS, A. (1979). *Acta Cryst.* B**35**, 1804–1809.
WITH, G. DE, FEIL, D. & BAERENDS, E. J. (1975). *Chem Phys. Lett.* **34**, 497–499.
ZIEGLER, G. E. (1935). *Z. Kristallogr.* **90**, 95.

Acta Cryst. (1983). C**39**, 936–939

La Structure de l'Orthophosphate Triple de Magnésium et de Sodium, $NaMg_4(PO_4)_3$

PAR M. BEN AMARA, M. VLASSE, R. OLAZCUAGA, G. LE FLEM ET P. HAGENMULLER

Laboratoire de Chimie du Solide du CNRS, Université de Bordeaux I, 351 *cours de la Libération*, 33405 *Talence CEDEX, France*

(*Reçu le* 19 *juillet* 1982, *accepté le* 6 *avril* 1983)

Abstract. $M_r = 405{\cdot}2$, orthorhombic, *Pnma*, $a = 9{\cdot}883\ (2)$, $b = 6{\cdot}345\ (2)$, $c = 15{\cdot}240\ (3)$ Å, $V = 955{\cdot}7$ Å^3, $Z = 4$, $D_m = 2{\cdot}84 \pm 0{\cdot}05$, $D_x = 2{\cdot}82$ Mg m^{-3}, room temperature, $\lambda(\text{Mo } K\alpha_1) = 0{\cdot}70942$ Å, $\mu = 10{\cdot}16$ cm^{-1}, $F(000) = 800$. The structure has been refined with 1325 single-crystal diffractometer data to $R = 0{\cdot}053$. The three-dimensional lattice is made up of isolated $[PO_4]$ tetrahedra linked together by Mg and Na atoms. A strong $[MgO_5]$ polyhedral sublattice appears with voids occupied by the Na atoms.

Introduction. Les besoins en matériaux nouveaux susceptibles de jouer le rôle de 'structures d'hôte' pour des ions optiquement actifs ou répondant à des critères de mobilité ionique ont conduit à l'étude d'un certain nombre d'orthovanadates et d'orthophosphates.

Divers auteurs (Hagenmuller & Van Gool, 1978; Goodenough, Hong & Kafalas, 1976) ont montré que certains matériaux à squelette tridimensionnel pouvaient comporter des ions alcalins à mobilité élevée.

Les composés comportant des groupements fortement covalents tels que SiO_4^{4-}, PO_4^{3-} ou VO_4^{3-} possèdent souvent de tels réseaux tridimensionnels. Un certain nombre de ces structures ont été étudiées, en particulier celles qui répondaient à la formule générale $AB_4(XO_4)_3$ (A = Na, K; B = Cd; X = P, V): $KCd_4(VO_4)_3$ (Holt, Drai, Olazcuaga & Vlasse, 1977), $NaCd_4(VO_4)_3$ (Ben Amara, Vlasse, Olazcuaga & Le Flem, 1979), $NaCd_4(PO_4)_3$ (Ben Amara, Olazcuaga, Le Flem & Vlasse, 1979).

En vue de mettre en évidence des caractéristiques structurales conduisant aux propriétés physiques recherchées nous avons entrepris l'étude de la structure de $NaMg_4(PO_4)_3$.

Partie expérimentale. $NaMg_4(PO_4)_3$ est obtenu à partir d'un mélange de carbonate de sodium, de carbonate de magnésium et de phosphate diammonique en proportions stochiométriques selon la réaction:

$$Na_2CO_3 + 8MgCO_3 + 6(NH_4)_2HPO_4 \rightarrow 2NaMg_4(PO_4)_3 + 9CO_2 + 12NH_3 + 9H_2O.$$

La réaction est terminée après trois calcinations de 4 h à 523 K, de 15 h à 873 K et de 15 h à 1173 K entrecoupées de broyages. Le produit obtenu est blanc et non hygroscopique.

Des monocristaux ont été obtenus par refroidissement lent (10 K h^{-1}) jusqu'à 773 K d'un bain fondu à 1273 K de 10g de $NaMg_4(PO_4)_3$.

L'analyse radiocristallographique: chambre de Weissenberg et goniomètre de précession, réflexions observées $hk0$: $h = 2n$ et $0kl$: $k + l = 2n$, groupes d'espace possibles *Pnma* ou $Pn2_1a$. Ces résultats sont conformes à ceux annoncés (Majling & Hanic, 1976).

Le monocristal choisi: parallélipipède, 0,14 × 0,13 × 0,09 mm, orienté selon l'axe c. Diffractomètre automatique Enraf–Nonius CAD-3 à trois cercles, radiation $K\alpha_1$ du molybdène ($\lambda = 0{,}70942$ Å), monochromateur de graphite, balayage multiple ($\theta/2\theta$) faite à l'aide d'un compteur à scintillations à une vitesse (2θ) 10° min^{-1}. L'intensité du fond continu a été déterminée de part et

0108-2701/83/080936-04$01.50